Dynamic variations of a convection flow reversal in the subauroral postmidnight sector as seen by the SuperDARN Hokkaido HF radar

Ryuho Kataoka,[1,2] Nozomu Nishitani,[2] Yusuke Ebihara,[3] Keisuke Hosokawa,[4] Tadahiko Ogawa,[5] Takashi Kikuchi,[2] and Yoshizumi Miyoshi[2]

Received 6 August 2007; revised 2 October 2007; accepted 15 October 2007; published 14 November 2007.

[1] The SuperDARN Hokkaido HF radar, capable of measuring the subauroral ionospheric plasma convection especially during storms, has been in continuous operation since the beginning of December 2006. We report the first two-dimensional observation of a dynamic variation of convection flow reversal in subauroral postmidnight sector during the storm main phase on 29 January 2007. The flow reversal region is extended over 20° in longitude and 5° in latitude, lasting for about 10–15 min, and the maximum flow speed is about 0.5–1.0 km/s. The flow reversal structure is reasonably reproduced by the ring current simulation coupled with the ionosphere, suggesting that it is produced by the region 2 field-aligned current associated with the ring current enhancement during the storm main phase. The dynamic variation of the flow reversal structure is interpreted as a transient eastward extension of the elongated dusk convection cell to the postmidnight and equatorward of the dawn cell, associated with the variation of the ring current whose structure is controlled by the interplanetary magnetic field and solar wind dynamic pressure. It is suggested that the ring current variation is highly coupled with the interplanetary parameters and is much more complicated than ever thought.
Citation: Kataoka, R., N. Nishitani, Y. Ebihara, K. Hosokawa, T. Ogawa, T. Kikuchi, and Y. Miyoshi (2007), Dynamic variations of a convection flow reversal in the subauroral postmidnight sector as seen by the SuperDARN Hokkaido HF radar, *Geophys. Res. Lett.*, *34*, L21105, doi:10.1029/2007GL031552.

1. Introduction

[2] The subauroral ionosphere and the electric field therein are one of the most important subjects for space weather research because they are directly coupled to ring current particles. During magnetic storms, it may be possible that the dynamic variation of the ring current particles transiently produce strong subauroral electric fields via magnetosphere-ionosphere coupling. In fact, complicated convection patterns, such as an elongated dusk cell extended to the equatorward edge of the dawn cell, were actually observed by DMSP satellites during a superstorm [*Ebihara et al.*, 2005], although the satellite observation cannot discriminate the temporal/spatial variations of the flow reversals. The present paper addresses this issue by using the two-dimensional observation of storm-time subauroral electric fields obtained by the newly constructed SuperDARN Hokkaido radar. The purpose of this short report is to show evidence for the dynamic variation of a convection flow reversal in response to the solar wind variation in subauroral postmidnight sector during a moderate magnetic storm on 29 January 2007. The observed dynamic variation of the flow reversal is compared with the simulation results from the Comprehensive Ring Current Model (CRCM) [*Fok et al.*, 2001] to understand the generation mechanism.

2. Observational Results

[3] The SuperDARN Hokkaido HF radar is capable of measuring the subauroral ionospheric plasma flow especially during magnetic storms when the auroral oval expands to lower latitude than the fields-of-view of the high-latitude SuperDARN radars. The Hokkaido radar was constructed in Rikubetsu town, Hokkaido, Japan at 43.53°N and 143.61°E in geographic coordinates. The magnetic latitude (MLAT) is 36.46° and the *L*-value is 1.55 (c.f., the Wallops radar [e.g., *Greenwald et al.*, 2006] is at magnetic latitude of 49.4°). The Hokkaido radar has been in continuous operation since the beginning of December 2006. The field-of-view (FOV) of the Hokkaido radar extends from 40° to 65° MLAT. A complete scan of the FOV is achieved every 1.0 min with the transmission frequency of ~11 MHz on 29 January 2007.

[4] The line-of-sight Doppler velocity observation of the flow reversal region is summarized in Figure 1. The spatial extent of the flow reversal region is about 1.5 hour in magnetic local time (MLT) and 5° in MLAT. Red and blue colors correspond to the line-of-sight velocity away from and toward the radar, respectively. The maximum flow speed is estimated as 0.5–1.0 km/s, simply assuming that the flow direction were azimuthal. Actually, the line-of-sight Doppler speed basically becomes larger with increasing beam number, indicating that the azimuthal flow is a good assumption in this case. The flow reversal is located in subauroral latitudes, since the electron auroral images obtained by TIMED GUVI (http://guvi.jhuapl.edu/) at that time indicate that the equatorward boundary of the auroral oval at 1608 UT was located about 62°–63° MLAT around midnight (not shown), which is a few degrees poleward of

[1]Computational Astrophysics Laboratory, Institute of Physics and Chemical Research (RIKEN), Wako, Japan.
[2]Solar-Terrestrial Environment Laboratory, Nagoya University, Nagoya, Japan.
[3]Institute for Advanced Research, Nagoya University, Nagoya, Japan.
[4]Department of Information and Communication Engineering, University of Electro-Communications, Tokyo, Japan.
[5]Solar-Terrestrial Environment Laboratory, Nagoya University, Toyokawa, Japan.

0094-8276/07/2007GL031552

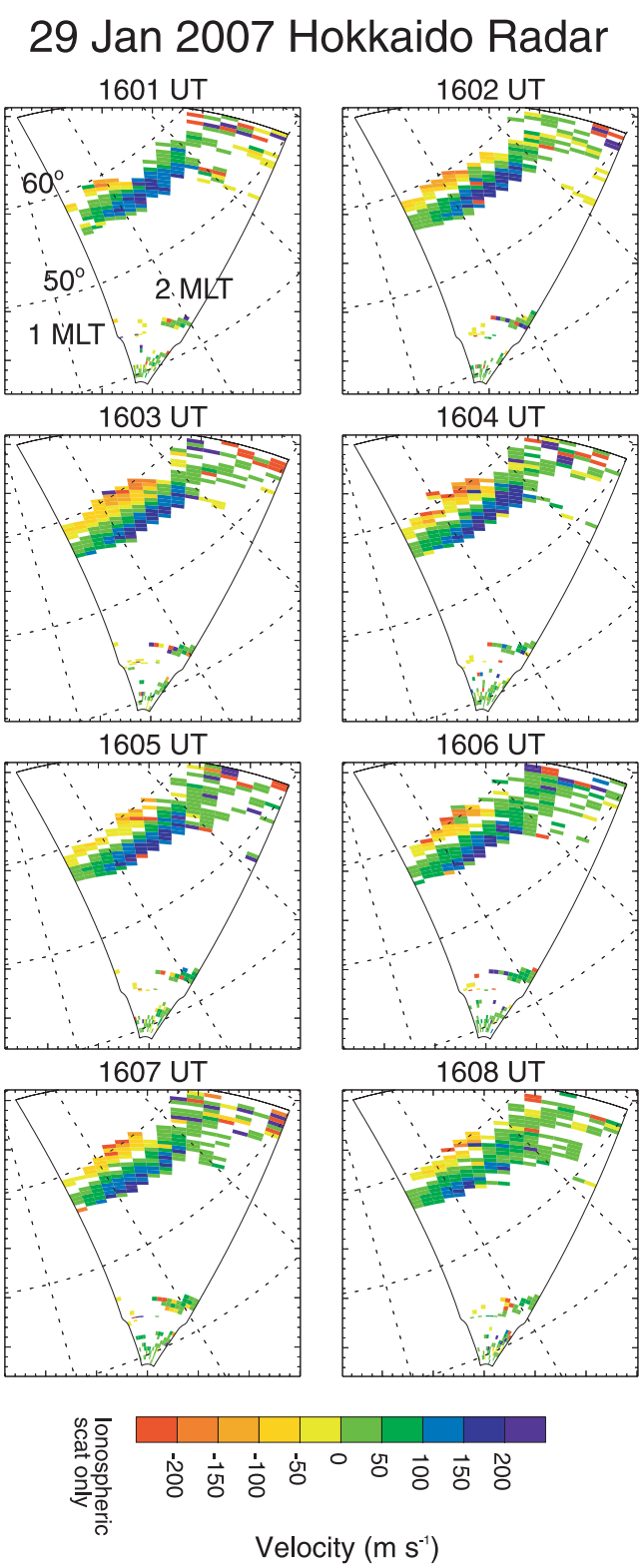

Figure 1. Line-of-sight Doppler velocity maps of the convection flow reversal in subauroral latitudes, color coded by warm (away from the radar) and cold (toward the radar) colors: from left to right of the field-of-view, the beam number increases from 0 to 15. The magnetic latitude and longitude are given in the Altitude Adjusted Corrected Geomagnetic Coordinate (AACGM) system.

the flow reversal. The flow reversal is a transient phenomenon showing a dynamic variation particularly in the east-west direction as shown in Figure 1: The flow reversal started to develop from westward edge of the FOV (55°–60° MLAT, 2.0 MLT) at 1601 UT, a beautiful flow reversal expands in longitude at 1603 UT, and the flow reversal started to fade out from eastward edge of the FOV (55°–60° MLAT, 2.5 MLT) at 1608 UT.

[5] The solar wind parameters were monitored by the Geotail satellite just upstream of the nominal bow shock in the vicinity of the subsolar point; (x, y, z) = (19.46, −0.07, −5.28) Re in GSE coordinate system at 1600 UT. The average time delay from Geotail to the inner magnetosphere for the three hour time interval is estimated to be about three min from the good correlation between the solar wind dynamic pressure at Geotail (Figure 2c) and the magnetic field Hp component (essentially parallel to Earth's rotation axis) at GOES 12 (Figure 2d) located at prenoon geosynchronous orbit; (x, y, z) = (5.96, −1.49, 2.43) Re in GSE coordinate system at 1600 UT. Since the GOES 12 is in the dayside magnetosphere, the increase and decrease of the Hp component indicate the compression and expansion of the magnetosphere, respectively. The solar wind speed is stable at about 600 km/s (not shown). The whole three hour time interval is a part of typical corotating interaction region with a strong interplanetary magnetic field (IMF) of up to 20 nT. The IMF B_X component (not shown) is rather stable at about −10 nT, compared to the other two components shown in Figures 2a and 2b. The effect of southward B_Z starting at ∼1600 UT (Figure 2b) appeared in the magnetosphere/ionosphere almost simultaneously as indicated by the enhancement of the PCN index (Figure 2f). Before the flow reversal event, the storm main phase started at ∼1400 UT, and a substorm was in the recovery phase after ∼1500 UT (Figure 2g). The Kp index during the three hour time interval was 5+.

[6] Figure 2h shows the line-of-sight Doppler velocity along the beam 5 for the time interval 1500–1630 UT. It is apparent that the flow reversal is found not only for the time interval 1600–1610 UT but also for the time interval 1540–1550 UT. As indicated by vertical dotted lines in Figure 2, the appearance of the flow reversals corresponds to the expansion of the magnetosphere (Figures 2d and 2e) due to the decrease of solar wind dynamic pressure (Figure 2c). The associated IMF variation would be positive B_Y enhancement (Figure 2a) for the first flow reversal event, and negative B_Z enhancement (Figure 2b) for the second flow reversal event.

[7] The NOAA POES-18 satellite crossed over the first flow reversal event at 1535–1537 UT. The ring current ions of 30–80 keV from the MEPED instrument and downward energy flux of auroral electrons of <20 keV from the TED instrument [*Evans and Greer*, 2000] are shown in Figures 3a and 3b, respectively. A value of 1 erg/cm^2 s of the downward energy flux is referred to as a rough threshold of visible aurora [*Yahnin et al.*, 1997]. From Figure 3b, the equatorward boundary of the auroral oval is located at about 60° MLAT and 1.8 MLT, at 1535–1536 UT, indicating that the flow reversal occurred in the subauroral region, consistent with the TIMED GUVI observation. The inner boundary of the ring current particles is located at about

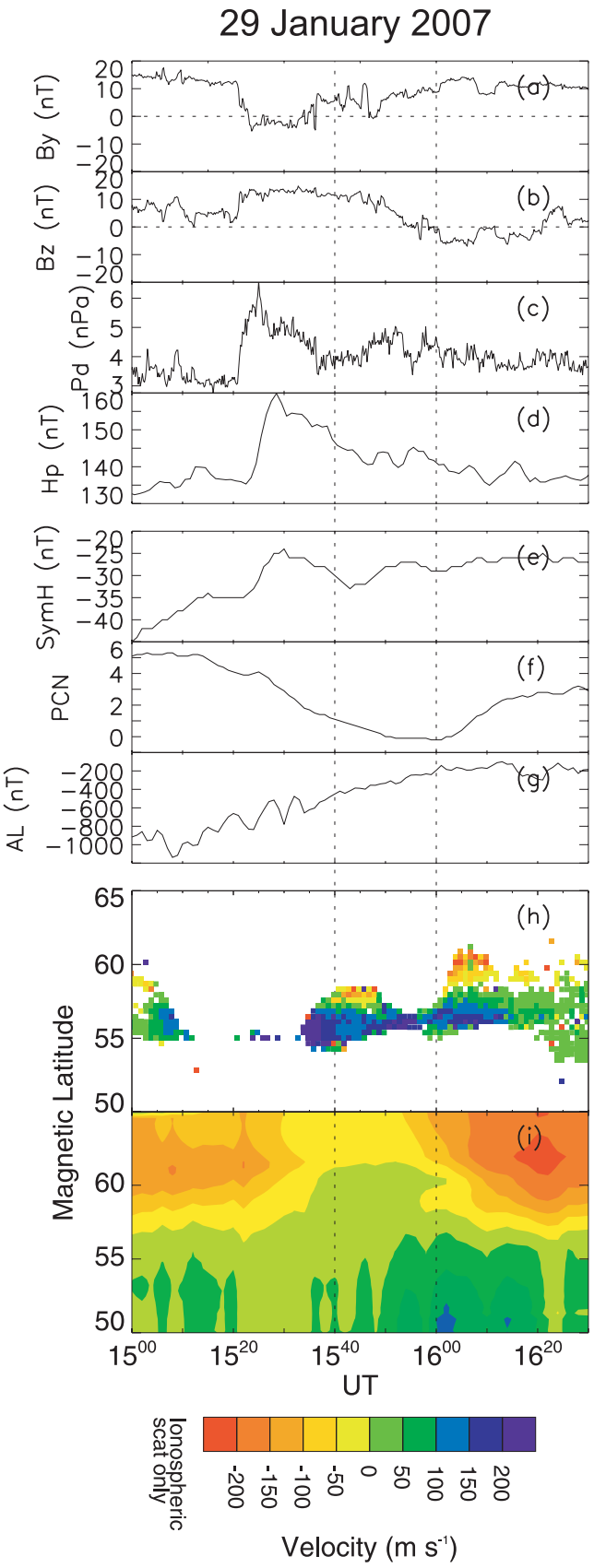

55° MLAT as shown in Figure 3a, implying that the flow reversal is overlapped with the ring current region.

3. Simulation Results

[8] In order to understand the generation mechanism of the flow reversal, we compare the observation results with the simulation results obtained from the CRCM [*Fok et al.*, 2001]. The high-latitude boundary of the CRCM convection pattern is given by the Weimer model [*Weimer*, 2005] as functions of IMF B_Y and B_Z, solar wind speed and density. The line-of-sight Doppler velocity along the beam 5 is obtained from the simulation as shown in Figure 2i. As a result, the flow reversal region appeared at ~1600 UT from 50° to 60° MLAT. Although the latitude of simulated reversal is a few degrees lower than observation of the second flow reversal event, the simulated flow speed is comparable to the observation, and the transient time scale of 10–15 min shows a nice agreement with the observation. In this simulation, the flow reversal is produced due to the increase of the ring current and the associated region 2 field-aligned current (R2FAC) flowing out of the postmidnight ionosphere, corresponding to the enhancement of the cross polar cap potential (CPCP) by the negative IMF B_Z. The relationship with the ring current is consistent with the observation by NOAA/POES as shown in Figure 3a.

4. Discussion

[9] The first flow reversal event does not appear in the simulation, implying that some different mechanism from the IMF effect is working for producing the first event. As a possibility, the temporarily expanding state of the magnetosphere may be associated with the appearance of the first flow reversal. The CRCM does not include the effect of the time-varying magnetic field strength in the inner magnetosphere, although the GOES 12 observation shows about 10% decrease of the total magnetic field at that time (Figure 2d). More sophisticated coupling codes of the global magnetohydrodynamic simulation and the ring current simulation incorporating the self-consistent background magnetic field are needed to reveal details of the mechanism of the inner magnetospheric response to the solar wind variations.

[10] There is a possibility that we are looking at the same phenomenon as reported by *Oksavik et al.* [2006], in which so-called subauroral ion drift (SAID) [e.g., *Karlsson et al.*, 1998; *Anderson et al.*, 2001] extended toward postmidnight sector. Also, *Baker et al.* [2007] showed a similar structure of tongue-like dusk convection cell extended equatorward of the nightside dawn cell. Based on an output from the CRCM simulation that shows how the pressure gradient

Figure 2. Summary plot for the time interval 1500–1630 UT during the storm main phase on 29 January 2007: (a) and (b) GSM Y and Z component of the IMF at Geotail, (c) solar wind dynamic pressure at Geotail, (d) magnetic field perpendicular to the GOES 12 orbital plane, (e) SYMH index, (f) PCN index, (g) real-time AL index, (h) observed line-of-sight Doppler velocity along the beam 5, and (i) simulated line-of-sight velocity along the beam 5.

induced field-aligned currents relate to the ionospheric flow patterns, Figure 4 shows a cartoon explaining the flow reversal structure during storms. The westward drift at the equatorward side of the flow reversal is interpreted as a part of the elongated dusk cell that expanded through midnight. The elongated dusk cell is driven by the R2FAC flowing out of the low conductivity ionosphere. The R2FAC is generated from the divergence of the ring current flowing azimuthally in the high-pressure region. As shown in Figure 1, the dynamic evolution of the flow reversal expands from west and retreats from east to west, consistent with the appearance and disappearance of the eastern edge of the elongated dusk cell into and out of the FOV, respectively. Thus, the results may imply that the evolution of the flow reversal responds directly to the inner magnetospheric plasma pressure, although it needs further study before such conclusion because there are other mechanisms at work in this local time/latitude sector leading to westward flow channels. In fact, similar flow reversals have been seen at the Millstone Hill IS rader and reported and alternate driving mechanisms discussed by *Huang et al.* [2001].

[11] In the above discussion, we implicitly assumed the appearance and subsequent disappearance of the backscattering irregularities was due to the formation and subsequent relaxation of an enhanced convection electric field. This is just for discussing in the simplest way, based on the idea that the strong electric field and the density gradient near the edge of the subauroral trough may be effective in producing the field-aligned irregularities (FAIs). The production of FAIs in the subauroral region is an interesting and important topic [e.g., *Greenwald et al.*, 2006], although detailed discussion on the FAI production itself is beyond the scope of this paper.

[12] The above results obtained in this paper suggest that the self-consistent current system including R2FAC produced by ring current particle dynamics coupled with the ionosphere is important to understand the electric fields in the subauroral region and the inner magnetosphere, especially during magnetic storms. Also, this paper demonstrates how the midlatitude SuperDARN HF radar works as a "Storm Radar" to see how the normal two-cell convection pattern is significantly modified and dynamically changing in response to the solar wind variation during storms. Such a dynamic variation of the subauroral convection pattern is never captured by satellite observation, and it reminds us of the advantage and importance of the ground-based instruments.

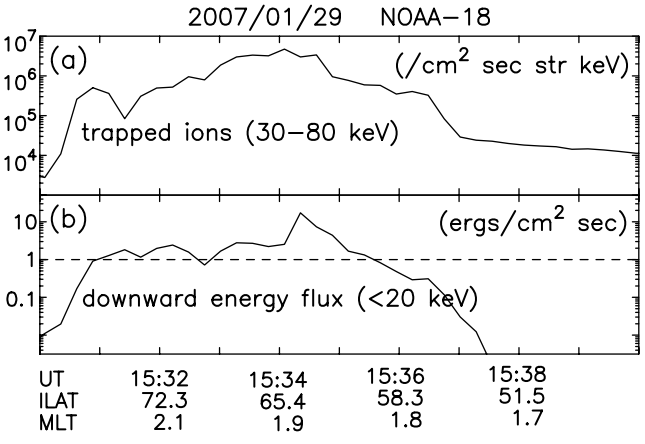

Figure 3. NOAA-POES 18 observations crossing over the flow reversal region: (a) trapped ions of 30–80 keV and (b) downward electron energy flux of <20 keV. The dashed line in the bottom panel shows the empirical reference value for the visible aurora.

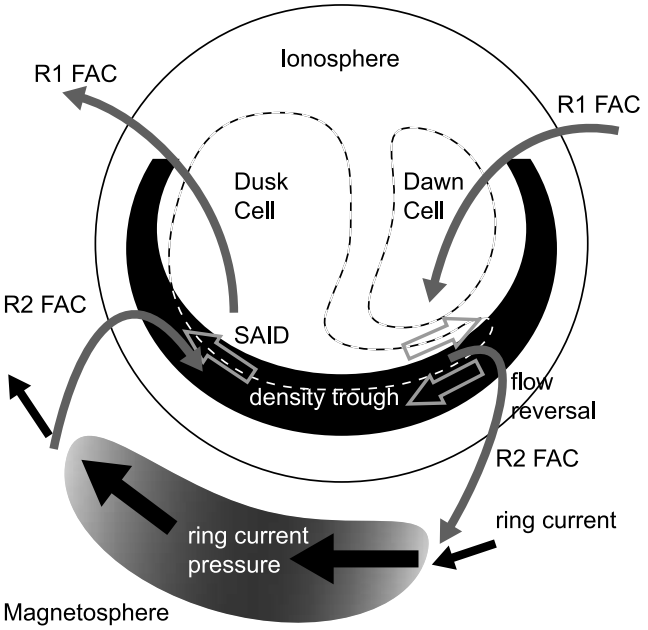

Figure 4. Illustration of the magnetosphere-ionosphere current system showing a possible generation mechanism of SAID and the flow reversal structure.

[13] **Acknowledgments.** The work by RK was supported by a research fellowship of the Japan Society for the Promotion of Science for Young Scientists and a research fellowship of Special Postdoctoral Research Program at RIKEN. The SYMH and AL indices were provided from Kyoto University, and the PCN index was provided from Danish Meteorological Institute. The POES and GOES data were provided from NOAA. Geotail MAG data were provided by T. Nagai and Geotail LEP data were provided by Y. Saito and T. Mukai through ISAS/JAXA.

References

Anderson, P. C., D. L. Carpenter, K. Tsuruda, T. Mukai, and F. J. Rich (2001), Multisatellite observations of rapid subauroral ion drifts (SAID), *J. Geophys. Res.*, *106*, 29,585–29,599.

Baker, J. B. H., R. A. Greenwald, J. M. Ruohoniemi, K. Oksavik, J. W. Gjerloev, L. J. Paxton, and M. R. Hairston (2007), Observations of ionospheric convection from the Wallops SuperDARN radar at middle latitudes, *J. Geophys. Res.*, *112*, A01303, doi:10.1029/2006JA011982.

Ebihara, Y., M.-C. Fok, S. Sazykin, M. F. Thomsen, M. R. Hairston, D. S. Evans, F. J. Rich, and M. Ejiri (2005), Ring current and the magnetosphere-ionosphere coupling during the superstorm of 20 November 2003, *J. Geophys. Res.*, *110*, A09S22, doi:10.1029/2004JA010924.

Evans, D. S., and M. S. Greer (2000), Polar orbiting environmental satellite space environment monitor: 2, Instrument description and archive data documentation, *NOAA Tech. Memo. OAR SEC-93*, Natl. Oceanic and Atmos. Admin., Boulder, Colo.

Fok, M.-C., R. A. Wolf, R. W. Spiro, and T. E. Moore (2001), Comprehensive computational model of Earth's ring current, *J. Geophys. Res.*, *106*, 8417–8424.

Greenwald, R. A., K. Oksavik, P. J. Erickson, F. D. Lind, J. M. Ruohoniemi, J. B. H. Baker, and J. W. Gjerloev (2006), Identification of the temperature gradient instability as the source of decameter-scale ionospheric irregularities on plasmapause field lines, *Geophys. Res. Lett.*, *33*, L18105, doi:10.1029/2006GL026581.

Huang, C., J. C. Foster, and J. M. Holt (2001), Westward plasma drift in the midlatitude ionospheric F region in the midnight-dawn sector, *J. Geophys. Res.*, *106*(A12), 30,349–30,362.

Karlsson, T., G. T. Marklund, L. G. Blomberg, and A. Mälkki (1998), Subauroral electric fields observed by the Freja satellite: A statistical study, *J. Geophys. Res.*, *103*, 4327–4341.

Oksavik, K., R. A. Greenwald, J. M. Ruohoniemi, M. R. Hariston, L. J. Paxton, J. B. H. Baker, J. W. Gjerloev, and R. J. Barnes (2006), First observations of the temporal/spatial variation of the sub-auroral polarization stream from the SuperDARN Wallops HF radar, *Geophys. Res. Lett.*, *33*, L12104, doi:10.1029/2006GL026256.

Weimer, D. R. (2005), Improved ionospheric electrodynamic models and application to calculating Joule heating rates, *J. Geophys. Res.*, *110*, A05306, doi:10.1029/2004JA010884.

Yahnin, A. G., V. A. Sergeev, B. B. Gvozdevsky, and S. Vennerstrom (1997), Magnetospheric source region of discrete auroras inferred from their relationship with isotropy boundaries of energetic particles, *Ann. Geophys.*, *15*, 943–958.

Y. Ebihara, Institute for Advanced Research, Nagoya University, Nagoya, 464-8601 Japan. (ebihara@stelab.nagoya-u.ac.jp)

K. Hosokawa, Department of Information and Communication Engineering, University of Electro-Communications, Tokyo, 182-8585 Japan. (hosokawa@ice.uec.ac.jp)

R. Kataoka, Computational Astrophysics Laboratory, RIKEN, Wako, 351-0198 Japan. (ryuho@riken.jp)

T. Kikuchi, Y. Miyoshi, and N. Nishitani, Solar-Terrestrial Environment Laboratory, Nagoya University, Nagoya, 464-8601 Japan. (kikuchi@stelab.nagoya-u.ac.jp; miyoshi@stelab.nagoya-u.ac.jp; nisitani@stelab.nagoya-u.ac.jp)

T. Ogawa, Solar-Terrestrial Environment Laboratory, Nagoya University, Toyokawa, 442-8507 Japan. (ogawa@stelab.nagoya-u.ac.jp)